An Approximate Solution to Some Ferrite Filled Waveguide Problems with Longitudinal Magnetization*

SHELDON S. SANDLER†

Summary—An approximate solution for the field structure and propagating modes in parallel plane, circular, and coaxial ferrite filled waveguide is presented. Bundles of plane waves are assumed to propagate in these structures which bounce back and forth along the guide. The solutions are classified into two types depending on the negative or positive equality of the incident and reflected waves. In the case of the circular guide the waves form a cone, and in the coaxial guide they form a frustum of a cone about the axis. The elemental plane waves are also assumed to satisfy Polder's relation and the boundary conditions at the guide walls. Simple relations are obtained with this equivalence for the propagation constant and the field. Comparison to rigorous theory is made in the case of the parallel plane and circular guide. Some experimental verification is presented for the completely filled coaxial waveguide.

Introduction

THE solution of the propagating modes in a general cylindrical guide has been given by Kales [1] and Suhl and Walker [2]. With these formulations the researcher is faced with an almost insurmountable computational problem for the propagation constants and the field configurations in practical waveguide structures. It is not the purpose of this paper to reformulate the problem, but rather to present an approximate method which will lend insight into the phenomenon and ease some of the computational difficulties.

The method is based on a well-known result in isotropically filled waveguide. The result shows that the solution to the rigorous boundary value problem in parallel-plate guide may be visualized as a set of plane waves bouncing back and forth along the guide. The results of using the plane wave picture are identical to the rigorous results. For example, in the cutoff condition the plane waves move at right angles to the longitudinal axis of the guide. It will be demonstrated that the same picture may be applied to a parallel-plate ferrite filled waveguide. Furthermore, the same method may be extended to the completely filled circular and coaxial waveguide.

The results of the approximate method will be compared to the rigorous results for the completely filled parallel-plate guide given by Brodwin [3] and the completely filled circular guide given by Gamo [4]. Since no results have been published on the completely-filled coaxial line, these results will be presented with some verification from experimental measurements.

* Received by the PGMTT, September 15, 1960; revised manuscript received, November 28, 1960. The research reported herein was supported in part by the AF Cambridge Res. Ctr., Air Res. and Dev. Command, under Contract AF 19(604)-5234 and in part by the Naval Bureau of Ships under Contract NObsr 77602.

† Electronic Communications Inc., Timonium, Md.

The Method

An explanation of the approximate method might best begin from a crude discussion of the most elementary isotropic waveguide, the parallel-plate guide. It has been shown by many authors that the rigorous solution is equivalent to a set of plane waves bouncing back and forth along the guide. Consider a plane wave impinging on a semi-infinite perfect conductor as shown in Fig. 1.

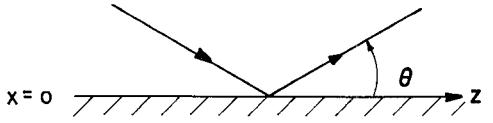

Fig. 1—Plane wave impinging on perfect conductor.

From geometrical considerations, the phase factors of the tangential incident and reflected waves of Fig. 1 are given by

$$E_i \sim \mathcal{E}_i e^{-j\beta \cos\theta z - j\beta \sin\theta x}$$

$$E_r \sim E_r e^{-j\beta \cos\theta z + j\beta \sin\theta x}. \tag{1}$$

Since the tangential components of the electric field must be zero at $x=0$ for all z, then $\mathcal{E}_i = -\mathcal{E}_r$ and

$$E_{\text{tang}} \sim \sin(\beta x \sin\theta) e^{-j\beta \cos\theta z}. \tag{2}$$

Eq. (2) represents a standing wave in the x direction and a traveling wave in the z direction. Note that another plate may be inserted at $x=a$ if

$$\beta a \sin\theta = v_m, \tag{3}$$

where

$$v_m = m\pi \qquad m = 1, 2, 3, \cdots. \qquad \text{(TM TYPE, "TMT")}$$

Eq. (3) may be shown to be identical to the rigorous expression for β derived from the boundary value problem. Similarly, for a TE type (TET) solution the phase factors of the incident and reflected H waves are given in the same form as (1). The boundary condition is then

placed on the normal component of H with the result

$$H_{\text{norm}} \sim \cos(\beta x \sin\theta) e^{-j\beta \cos\theta z}. \tag{4}$$

The above result was obtained by representing the incident and reflected H field in the form given by (1). In this case, the origin must be shifted to the center of the guide and the walls placed at $x = \pm a$ such that

$$\beta a \sin\theta = vl \tag{5}$$

where

$$vl = l\pi/2, \qquad l = 1, 3, 5$$

(TE TYPE, "TET").

The preceding discussion has been given purposely in a nonrigorous manner as an introducton to a more involved treatment. The general vector form of the incident and reflected waves of Fig. 1 is given by

$$\begin{aligned} \boldsymbol{E}_i &= (\boldsymbol{E}_{xi} + \boldsymbol{E}_{yi} + \boldsymbol{E}_{zi}) e^{-j\beta \cos\theta z - j\beta \sin\theta x} \\ \boldsymbol{E}_r &= (\boldsymbol{E}_{xr} + \boldsymbol{E}_{yr} + E_{zr}) e^{-j\beta \cos\theta z + j\beta \sin\theta x}. \end{aligned} \tag{6}$$

Two different types of solutions will be considered. For the first type the magnitude of the reflected components tangential to the metal guide walls will be equal in magnitude and sign to the incident tangential components. The second type has reflected components which are equal in magnitude and opposite in sign to the incident tangential components. These results are summarized below for the parallel-plate guide

$$\left.\begin{aligned} \boldsymbol{E}_{yi} &= \boldsymbol{E}_{yr} \\ \boldsymbol{E}_{zi} &= \boldsymbol{E}_{zr} \end{aligned}\right\} \text{TET} \tag{7}$$

$$\left.\begin{aligned} \boldsymbol{E}_{yi} &= -\boldsymbol{E}_{yr} \\ \boldsymbol{E}_{zi} &= -\boldsymbol{E}_{zr} \end{aligned}\right\} \text{TMT}. \tag{8}$$

Note that (7) corresponds to a boundary condition (b.c.) of type (5) and similarly (8) corresponds to (3).

Now consider the same waveguide completely filled with a ferrite characterized by a tensor permeability of the following form

$$\mathfrak{u} = \mu_0 \begin{bmatrix} \mu & -j\mu' & 0 \\ j\mu' & \mu & 0 \\ 0 & 0 & 1 \end{bmatrix}. \tag{9}$$

The particular solutions presented in this paper will consist of bundles of plane waves, satisfying boundary conditions of type (3) or (5) at the guide walls. The angle of propagation θ given by (3) or (5) must also be the angle θ for propagation of a plane wave in an infinite medium. The well-known result for the propagation of a plane wave in an infinite ferrite medium is due to Polder [5] and is summarized below for convenience.

Let $\hat{s}$ be the direction of the wave (see Fig. 2) and

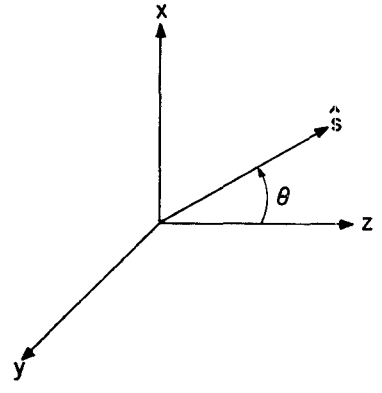

Fig. 2—Coordinate system for Polder's relation.

$\gamma = j\beta$, the corresponding propagation constant. Then Maxwell's equations reduce to

$$\gamma \hat{s} \times \boldsymbol{E} = -j\omega \mathfrak{u} \boldsymbol{h} \tag{10}$$

$$\gamma \hat{s} \times \boldsymbol{h} = j\omega \epsilon \boldsymbol{E}. \tag{11}$$

Eqs. (10) and (11) may be combined to give the following wave equation

$$\gamma^2[\hat{s}(\hat{s}\cdot\boldsymbol{h}) - \boldsymbol{h}] - \omega^2 \mathfrak{u} \epsilon \boldsymbol{h} = 0. \tag{12}$$

With the assumption $\boldsymbol{h} \neq 0$, (12) may be solved for γ^2, or

$$\gamma^2 = -\omega^2 \mu_0 \epsilon \frac{(\mu^2 - \mu - \mu'^2)\sin^2\theta + 2\mu \pm [(\mu^2 - \mu - \mu'^2)^2 \sin^4\theta + 4\mu'^2 \cos^2\theta]^{1/2}}{2[(\mu - 1)\sin^2\theta + 1]}. \tag{13}$$

Since the assumption is that plane waves are propagated, the value of θ in (13) must be identical to the value of θ in (3) or (5) or

$$\beta_i^2 \mu = \frac{(\mu^2 - \mu - \mu'^2)\left(\frac{v_m}{\beta_r a_r}\right)^2 + 2\mu \pm \left[(\mu^2 - \mu - \mu'^2)^2 \left(\frac{v_m}{\beta_r a_r}\right)^4 + 4\mu'^2\left(1 - \frac{v_m^2}{\beta_r^2 a_r^2}\right)\right]^{1/2}}{2\left[(\mu - 1)\left(\frac{v_m}{\beta_r a_r}\right)^2 + 1\right]} \tag{14}$$

where

$$\beta_r^2 = \beta^2/\omega^2\mu\mu_0\epsilon$$
$$a_r = a\omega\sqrt{\mu\mu_0\epsilon}.$$

Eq. (14) may be solved directly for β^2 in terms of μ, μ', v_m, and a. Note that the solution for β (13) is a function of the on-diagonal permeability μ. The results computed in this paper will assume a value of $\mu=1$, which is known to be a fairly good approximation for small anisotropies. It is important to note the simplicity of the expressions for the field and propagation constants compared with the classical results for the general case.

For $\mu=1$, (14) reduces to

$$2\beta_r^2 = -\left(\frac{\mu'}{\mu}\right)^2 \frac{v_m^2}{\beta_r^2 a_r^2} + 2 \pm \left[\left(\frac{\mu'}{\mu}\right)^4 \left(\frac{v_m}{\beta_r a_r}\right)^4 + 4\left(\frac{\mu'}{\mu}\right)^2 \left(1 - \frac{v_m^2}{\beta_r^2 a_r^2}\right)\right]^{1/2}. \quad (15)$$

The individual plane wave components satisfying (12) must be investigated to see which are TMT or TET. These actual plane wave components may be computed from (12) arranged in the matrix form given by

$$\begin{bmatrix} \gamma^2\cos^2\theta+\omega^2\mu\mu_0\epsilon & -j\omega^2\mu'\mu_0\epsilon & -\gamma^2\sin\theta\cos\theta \\ j\omega^2\mu'\mu_0\epsilon & \gamma^2+\omega^2\mu\mu_0\epsilon & 0 \\ -\gamma^2\sin\theta\cos\theta & 0 & \gamma^2\sin^2\theta+\omega^2\mu_0\epsilon \end{bmatrix} \begin{Bmatrix} h_x \\ h_y \\ h_z \end{Bmatrix} = 0. \quad (16)$$

The result (13) was found by noting that with $h\neq 0$ the determinant of the coefficients must be zero. The result gave two possible values of γ^2, γ_+^2 and γ_-^2. In general the determinant of (16) is of rank two, which is one less than the number of unknowns. The values of the h's in (16) are proportional to the cofactors of the coefficients in any row of the matrix (16).

The following three sets of polarization vectors represent three possible solutions

$$\begin{aligned} h_x &= C_1(\gamma^2+\omega^2\mu\mu_0\epsilon)(\gamma^2\sin^2\theta+\omega^2\mu_0\epsilon) \\ h_y &= C_1(j\omega^2\mu'\mu_0\epsilon)(\gamma^2\sin^2\theta+\omega^2\mu_0\epsilon) \\ h_z &= C_1(\gamma^2+\omega^2\mu\mu_0\epsilon)(\gamma^2\sin\theta\cos\theta), \end{aligned} \quad (17)$$

$$\begin{aligned} h_x &= C_2(-j\omega^2\mu'\mu_0\epsilon)(\gamma^2\sin^2\theta+\omega^2\mu_0\epsilon) \\ h_y &= C_2\{(\gamma^2\cos^2\theta+\omega^2\mu\mu_0\epsilon)(\gamma^2\sin^2\theta+\omega^2\mu_0\epsilon) \\ &\qquad -\gamma^4\sin^2\theta\cos^2\theta\} \\ h_z &= C_2(\gamma^2+\omega^2\mu\mu_0\epsilon)(\gamma^2\sin\theta\cos\theta), \end{aligned} \quad (18)$$

$$\begin{aligned} h_x &= C_3(\gamma^2+\omega^2\mu\mu_0\epsilon)(\gamma^2\sin\theta\cos\theta) \\ h_y &= C_3(j\omega^2\mu'\mu_0\epsilon)(\gamma^2\sin\theta\cos\theta) \\ h_z &= C_3\{(\gamma^2+\omega^2\mu\mu_0\epsilon)(\gamma^2\cos\theta+\omega^2\mu\mu_0\epsilon) \\ &\qquad -(\omega^2\mu'\mu_0\epsilon)^2\}. \end{aligned} \quad (19)$$

Kales[1] has shown that at the cutoff condition (*i.e.*, $\theta=\pi/2$) the classical hybrid solution reduces to the normal TE and TM waves. The plane wave solutions (17)–(19) will be examined near cutoff. For the case $\theta=\pi/2$, $\gamma^2=-\omega^2\mu_0\epsilon$ and the only nonzero solution is (19). The E and H components of this wave are shown in Fig. 3. This wave reduces to the TE-type wave at cutoff. On the other hand, if $\theta=\pi/2$ and $\gamma_+^2=-\omega^2\mu_0\epsilon(\mu^2-\mu'^2)/\mu$ then (17) and (18) reduce to the TMT wave shown in Fig. 4.

With $\theta<\pi/2$ both the γ_+^2 and γ_-^2 waves may be shown to satisfy TMT or TET b.c. with some degree of approximation. The degree of satisfaction of the b.c. of the correct type is found by noting the phase and

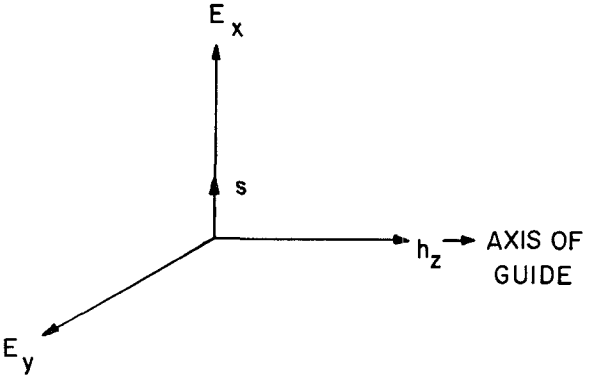

Fig. 3—Components of γ^2 wave at cutoff.

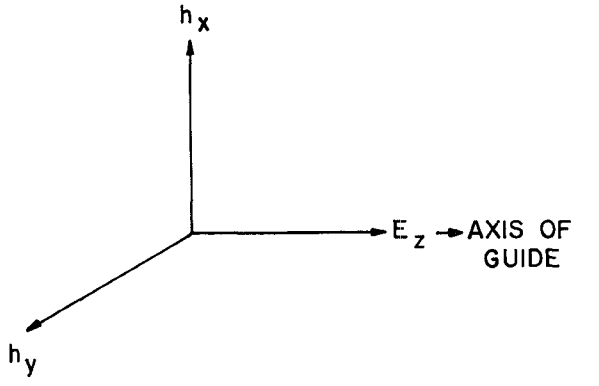

Fig. 4—Components of γ_+ wave at cutoff.

[1] Kales [1], *op. cit.*, p. 605.

magnitude of the incident and reflected tangential waves. All TMT waves must satisfy (8) and TET waves must satisfy (7). The electric field is easily found from (11) or

$$\boldsymbol{E} = \frac{\gamma}{j\omega\epsilon}\,\hat{s} \times \boldsymbol{h}$$

$$\boldsymbol{E} = \frac{\gamma}{j\omega\epsilon}\,[-\cos\theta h_x\hat{x} + (h_x\cos\theta - h_z\sin\theta)\hat{y} + h_y\sin\theta\hat{z}]. \quad (20)$$

The problem of satisfying (7) or (8) reduces to the determination of the evenness or oddness of the tangential E field of a particular solution. For example the TET solution (19) has the following properties for $\theta < \pi/2$

$$E_{yi} = -E_{yr}$$
$$E_{zi} = +E_{zr}. \quad (21)$$

Note that the E_z components satisfy TET b.c. for all values of θ while the E_y components do not satisfy the b.c. Consider now the TMT particular solution (18) where

$$E_{yi} = +E_{yr}$$
$$E_{zi} = -E_{zr}. \quad (22)$$

Note that in this case the E_z component satisfies the TMT b.c., and the E_y component does not satisfy the b.c. The behavior of the E_y component at the boundary must be investigated further by finding the ratio of E_y to E_z. This ratio may be computed from (20) with (17)–(19). The results for some representative values shown in Figs. 5 and 6 yield the ratio $(E_y/E_z) \leq 0.07$. For each solution it is necessary to check this ratio as a basis for estimating the accuracy of the results.

Brodwin has shown that there are certain critical spacings for each mode. From (3) and (5) it is really seen that for each mode

$$\beta_r x_r \geq (2m-1)\pi/2 \qquad m = 1, 2, 3 \cdots \text{TET} \quad (23)$$
$$\beta_r x_r \geq m\pi \qquad m = 1, 2, 3 \cdots \text{TMT} \quad (24)$$

where

$$\beta_z = \beta_r \cos\theta.$$

The critical spacings are given by the equalities in (23) and (24), since at cutoff

$$\sin\theta = 1 = v_m/\beta_r x_r. \quad (25)$$

Substitution of (25) in (13) gives, for the critical spacing,

$$x_r^{\text{crit}} = \frac{v_m}{\left[1 - \frac{\mu'^2}{\mu^2}\right]^{1/2}} \quad \text{TMT}. \quad (26)$$

Eq. (26) was derived with the plus sign in (13); application of the negative sign shows that

$$x_r^{\text{crit}} = v_m \quad \text{TET}. \quad (27)$$

Eq. (26) agrees exactly with Brodwin's equation (9). The critical spacing given by (27) is identical to the critical spacing in an isotropic waveguide. Note also that for the lowest-order plane wave modes to propagate in this type of structure β_r and X_r must satisfy

$$\beta_r x_r \geq \pi/2 \quad \text{TET}$$
$$\beta_r x_r \geq \pi \quad \text{TMT}.$$

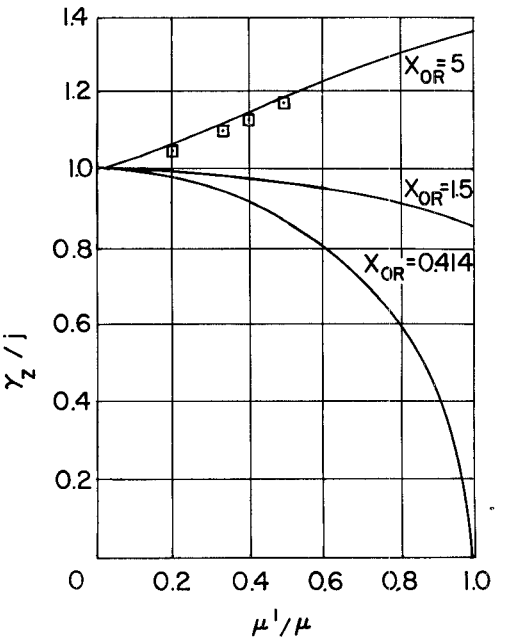

Fig. 5—Propagation constants of parallel-plane guide as a function of the anisotropy.

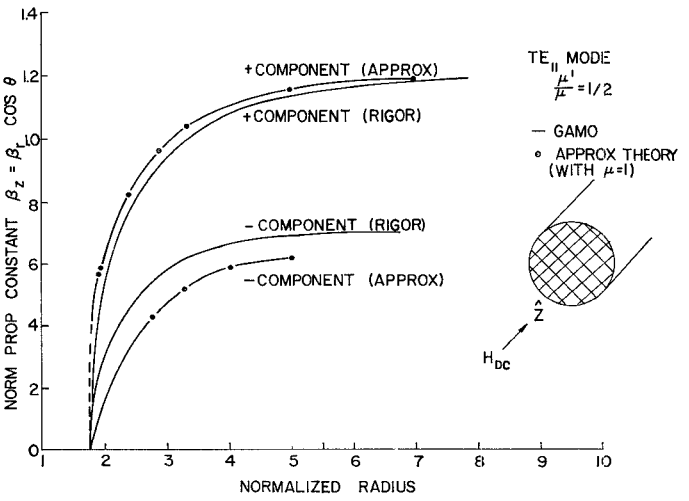

Fig. 6—Propagation constant of circular guide as a function of the radius ($\mu'/\mu = \frac{1}{2}$).

The above picture of a bundle of plane waves bouncing back and forth along the ferrite filled guide may be extended to circular structures. As a second application of the method, consider the circular guide in Fig. 7.

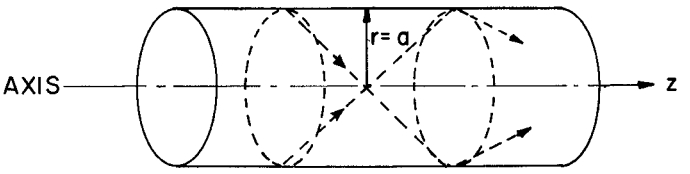

Fig. 7—Plane waves in circular guide.

In the case of the circular guide the bundle of plane waves forms a cone about the guide axis. For isotropically filled guide Schelkunoff [7] has shown that it is possible to express guided waves above cutoff as bundles of plane waves repeatedly reflected from the cylindrical boundary. A somewhat similar approach will be taken in this paper. Let the amplitude of the element incident tangential wave be $\mathcal{E}_{ti}(\alpha)d\alpha$ and reflected wave $\mathcal{E}_{tr}(\alpha)d\alpha$, then the total tangential field, E_t, is given by

$$E_t \sim e^{-j\beta z \cos\theta}\left\{\int_0^{2\pi} \mathcal{E}_{ti}(\alpha)e^{-j\beta(x\cos\alpha+y\sin\alpha)\sin\theta}d\alpha + \int_0^{2\pi} \mathcal{E}_{tr}(\alpha)e^{+j\beta(x\cos\alpha+y\sin\alpha)\sin\theta}d\alpha\right\}. \quad (28)$$

The first type of solution under consideration will have an elemental wave variation given by

$$\mathcal{E}_{ti} = E_0 e^{in\alpha} = \mathcal{E}_{tr}(\alpha) \quad \text{TMT} \quad (29)$$

where n is an integer. With (29) in (28) it follows that

$$E_t \sim E_0 e^{-j\beta z\cos\theta}\int_0^{2\pi} \cos\left[\beta\rho\sin\theta\cdot\cos(\phi-\alpha) - n\alpha\right]d\alpha, \quad (30)$$

where

$$\rho\cos(\phi-\alpha) = x\cos\alpha + y\sin\alpha.$$

The integration of (30) is readily performed with the result

$$E_t \sim 2E_0 e^{-j\beta z\cos\theta}\begin{Bmatrix}\sin n\phi\\ \cos n\phi\end{Bmatrix} J_n(\beta\rho\sin\theta). \quad (31)$$

The b.c. is that (31) be zero at the surface of a perfectly conducting cylinder of radius a, or

$$J_n(\beta a\sin\theta) = 0,$$

or

$$\beta a\sin\theta = v_m, \quad \text{where} \quad v_1 = 383,\ v_2 = 7.02, \text{ etc.} \quad (32)$$

The TET solution is constructed by considering elemental waves given by

$$\mathcal{E}_{ti}(\alpha) = E_0\cos(\phi-\alpha)e^{in\alpha} = -\mathcal{E}_{tr}(\alpha) \quad \text{TET.} \quad (33)$$

The odd symmetry of the incident and reflected waves in (33) result in a total tangential field given by (28) or

$$E_t \sim E_0 e^{-j\beta z\cos\theta}\int_0^{2\pi}\cos(\phi-\alpha)\cdot\sin\left[\beta\rho\sin\theta\cos(\phi-\alpha) - n\alpha\right]d\alpha$$

$$E_t \sim 2E_0 e^{-j\beta z\cos\theta}\begin{Bmatrix}\sin n\phi\\ \cos n\phi\end{Bmatrix} J_n'(\beta\rho\sin\theta). \quad (34)$$

Again, the b.c. is that (34) be zero at the surface of a perfectly conducting cylinder of radius a, or

$$J_n'(\beta a\sin\theta) = 0 \quad (35)$$

or

$$\beta a\sin\theta = v_m$$

where

$$v_1 = 1.84 \qquad v_2 = 5.34, \text{ etc.}$$

Note that the definition of the wave types has been changed for the round guide in order to preserve internal consistency. As in the case of the parallel-plane guide the assumed TET and TMT polarizations do not agree exactly with (33) or (29). The TET solution in the circular guide has E_z satisfied identically and E not satisfied. Similarly an examination of (18), (20) and (29) shows that for the TMT solution E_z is satisfied and E_ϕ is not. As in the case of the parallel-plate guide the ratio of the unsatisfied to the satisfied component must be negligible for a valid solution.

Since each plane wave in the bundle must satisfy Polder's relation, then (15) applies in this case with v_m given by (32) or (34). For each value of v_m, two values of β_r are obtained, and the critical radii are given by

$$a^{\text{crit}} = \frac{v_m}{[1-(\mu'^2/\mu^2)]^{1/2}} \quad \text{TMT} \quad (36)$$

$$a^{\text{crit}} = v_m \quad \text{TET.} \quad (37)$$

As a further application of the method, consider the coaxial line shown in Fig. 8. In this case one set of plane waves of the type (28) is not able to satisfy the boundary condition at $r=a$ and $r=b$.

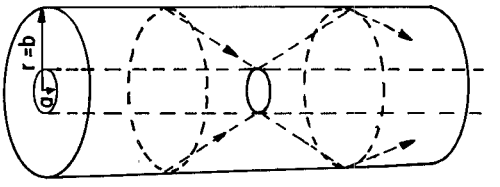

Fig. 8—Plane waves in coaxial guide.

In order to generate a second independent solution for the coaxial region, a new set of plane wave components must be found. These plane wave components will differ in amplitude from the plane wave components in (29) and (33). The second independent Bessel solution is well known (*i.e.*, the Neuman function solution). Here the problem is to represent the second bundle of waves as a Neuman function. The physical interpretation of the method in this paper is best preserved by working in the real domain. Consider the following representation of the Neuman function:

$$N_n(z) = \lim_{\nu \to n} \left\{ \frac{\partial J_\nu(z)}{\partial \nu} - (-1)^n \frac{\partial J_{-\nu}(2)}{\partial \nu} \right\}. \quad (38)$$

Now, from the integral representation

$$J_{\pm n}(z) = \frac{j^{\pm n}}{2\pi} \int_0^{2\pi} e^{\pm jn\psi} e^{+jz \cos \psi} d\psi \quad (39)$$

it follows

$$\frac{\partial J_{\pm \nu}(\partial)}{\partial \nu} = \frac{j^{\pm \nu}}{2\pi} \int_0^{2\pi} \pm j\psi e^{\pm j\nu\psi} e^{+jz \cos \psi} d\psi. \quad (40)$$

With (40) in (38) the Neuman function may be given in the form

$$N_n(z) = \lim_{\nu \to n} \frac{1}{2\pi} \left\{ \int_0^{2\pi} [j^{(1-n)} e^{jn\psi} - (-1)^n j^{-(1-n)} e^{-j\nu\psi}] \cdot e^{jz \cos\psi} d\psi \right.$$

$$N_n(z) = \frac{j^{3n+1}}{2\pi} \int_0^{2\pi} \psi \cos n\psi e^{jz \cos \psi} d\psi. \quad (41)$$

In other words, to obtain the second independent Bessel solution in a circular region the elemental plane waves must have amplitudes which vary as

$$\psi \cos \psi. \quad (42)$$

Returning to the TMT solution, the elemental incident and reflected waves have amplitudes given by

$$\mathcal{E}_{ti} = E_1(\phi - \alpha) \cos n\phi e^{jn(\phi - \alpha)} = \mathcal{E}_{tr} \quad \text{TMT}. \quad (43)$$

Substituting (43) in (28) and performing the integration, it follows that

$$E_t \sim \cos n\phi \{ E_0 J_n/\beta\rho \sin \theta) + E_1 N_n(\beta\rho \sin \theta) \}. \quad (44)$$

The b.c. are applied at $r = a$ and $r = b$, and noting that E_0 and E_1 are not identical zero it follows that

$$J_n(\beta a \sin \theta) N_n(\beta b \sin \theta) - J_n(\beta b \sin \theta) N_n(\beta a \sin \theta) = 0. \quad (45)$$

Without belaboring the point, the TET solution is generated by finding the elemental plane-wave components which integrate to form the derivative of the Neuman function. The propagation constant β is then given as a solution of the determinantal equation

$$J_n'(\beta a \sin \theta) N_n'(\beta b \sin \theta) - J_n'(\beta b \sin \theta) N_n'(\beta a \sin \theta) = 0. \quad \text{TET}. \quad (46)$$

Again as in the case of the circular guide, (45) and (46) are used in conjunction with Polder's relation (15) to determine the permissible values of β. Fortunately, all of the determinantal equations for β are identical to the isotropic case and have been solved for a wide variety of cases.

Theoretical and Experimental Results

Parallel-Plate Guide

Brodwin [3] has made some computations of the propagation constant and critical spacings of ferrite-filled parallel-plate guide. These results are given as a function of the anisotropy (μ'/μ) and were computed from the classical formulation. Brodwin's computation of β_z as a function of (μ'/μ) for different values of normalized spacing X_{0r} is shown in Fig. 5. The results apply to the odd quasi-TE, even quasi-TM and quasi-TEM modes. As a comparison the variation of β_z was calculated as a function of (μ'/μ) for a normalized spacing of $X_{0r} = 5$ from (15) and (23). Eq. (15) was solved by separating the equality into two parts, y_1 and y_2, where

$$y_1 = 2\beta_r^2 + \left(\frac{\mu'}{\mu}\right) \frac{v_n^2}{\beta_r^2 x_{0r}^2} - 2$$

$$y_2 = \left[\left(\frac{\mu'}{\mu}\right)^4 \frac{v_m^4}{\beta_r^4 x_{0n}^4} + 4\left(\frac{\mu'}{\mu}\right)^2 \left(1 - \frac{v_m^2}{\beta_r^2 x_{0r}^2}\right) \right]^{1/2}. \quad (47)$$

The value of β_z is found by multiplying the value of β_r by $\cos\theta = [1 - (v_m/\beta_r X_{0r})^2]^{1/2}$. The correct value of β_r was determined graphically from the equality $y_1 = y_2$. The quantitative agreement in Fig. 5 is excellent. The equation for the critical spacing (26) agrees exactly with Brodwin's (9) and was not plotted for comparison.

Circular Waveguide

Gamo investigated the propagation constant of ferrite filled circular guide for specific values of anisotropy. For a value of $(\mu'/\mu) = 1/2$, the propagation constant is plotted as a function of the radius in Fig. 6. Gamo's quasi-TE_{11} mode corresponds to the TET_{11} mode. Note that the behavior of the approximate solution is very close to the rigorous solution. Note that the TET_{11} cutoff may be defined for the minus component only. However, the plus component has the correct behavior near cutoff.

Coaxial Waveguide

No classical theoretical results were available to compare the approximate theory. An experimental model was constructed to test the theory and is shown in Figs. 9 and 10. A length of ferrite[2] 0.500 inch O.D.$\times$0.040 inch ID$\times$0.810 inch was placed between two stycast ($\varepsilon = 12$) pieces. The center conductor extended through

[2] Trans-Tech TT1-105.

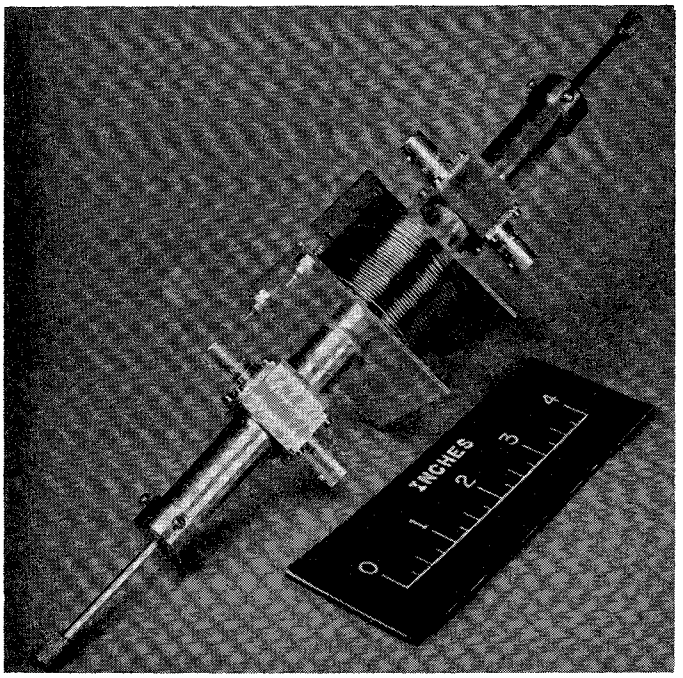

Fig. 9—Experimental device for measuring Faraday rotation in coaxial waveguide.

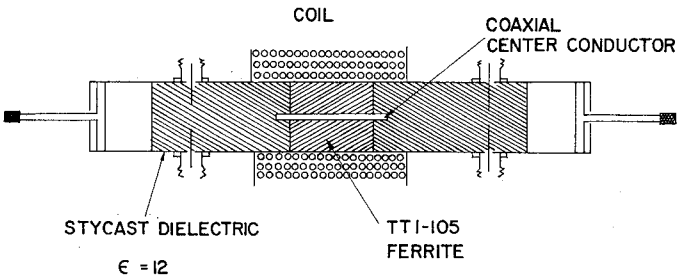

Fig. 10—Cross section of experimental coaxial rotator shown in Fig. 9

the ferrite and a short distance into the stycast pieces. Two probes were driven 180 electrical degrees out of phase to excite the TE_{11} mode in the completely stycast filled section of the guide. The guide was constructed so as to pass the TE_{11} mode and reject the next highest mode. Hopefully, the comparable TE_{11} mode was excited in the ferrite. Two other probes were mechanically fixed at the receiver end of the guide structure and lined up to the driven probes. The receiver probes were tuned for maximum output at 6000 Mc input with no applied field. The longitudinal magnetic field was then increased until the receiver output was a minimum. Filmohm resistance cards were placed at both ends of the unit in the dielectric pieces. These cards absorb the cross component of the RF energy when the magnetic field is applied. This value of field corresponded to 90° of Faraday rotation or

$$(1/2)(\beta_+ - \beta_-)l = \pi/2$$

or

$$(\beta_+ - \beta_-) = 0.206\beta_0. \tag{48}$$

Values of β_+ and β_- were computed from (15) as a function of (μ'/μ). It was found that for the size of coaxial ferrite insert (*i.e.*, $D/d = 12.5$) a value of $(\mu'/\mu) = 0.20$ corresponded to $(\beta_+ - \beta_-) = 0.206\beta_0$.

In order to gain some check on the above value of (μ'/μ) the experimental value of applied field was substituted in Kittel's theoretical expressions to find the actual value of (μ'/μ). The following physical constants were used

$$\chi = 0.558^{(8)}$$

$$N_l = 2.51 \qquad N_t = 5.03^{(9)}$$

$$H_a = 215 \text{ oersteds}$$

$$\bar{\gamma} = 1.76 \times 10^7 \text{ raa/sec/oersted.} \tag{49}$$

The demagnetization factor N was calculated by assuming the center hole in the ferrite had a negligible effect.

The value of (μ'/μ) corresponding to the above constants was calculated from the following formula given by Hogan [10]

$$\frac{\mu'}{\mu} = \frac{(4\pi - N_t)M\bar{\gamma}\omega}{\omega_0^2 + (4\pi - N_t)\bar{\gamma}M\omega - \omega^2} \tag{50}$$

$$\frac{\mu'}{\mu} = 0.20 \tag{51}$$

The above value represents an excellent agreement with approximate theory considering the variation of H_a (*i.e.*, 5 per cent) and the value of N.

Acknowledgment

The author would like to acknowledge the helpful suggestions and encouragement given by Dr. M. L. Kales of the Naval Research Laboratory. He also wishes to express his appreciation to Dr. J. Wiltse of Electronic Communications Inc., for his assistance on the experimental aspects of the problem.

Bibliography

[1] M. L. Kales, "Modes in waveguide containing ferrites," *J. Appl. Phys.*, vol. 24, pp. 604–608; May, 1953.
[2] H. Suhl and L. R. Walker, "Topics in guided wave propagation through gyromagnetic media," *Bell Sys. Tech. J.*, vol. 33, pp. 575–659; May, 1954.
[3] M. E. Brodwin, "Propagation in ferrite-filled microstrip," IRE Trans. on Microwave Theory and Techniques, vol. MTT-6, pp. 150–155; April, 1958.
[4] H. J. Gamo, "The Faraday rotation of waves in a circular waveguide," *J. Phys. Soc. Japan*, vol. 8, pp. 176–182; March–April, 1953.
[5] D. Polder, "On the Theory of Ferromagnetic Research," *Phil. Mag.*, vol. 40, pp. 99–115; 1949.
[6] F. B. Hildebrand, "Methods of Applied Mathematics," Prentice-Hall Inc., New York, N. Y. p. 23; 1952.
[7] S. A. Schelkunoff, "Electromagnetic Waves," D. Van Nostrand Co., Inc., Princeton, N. J., pp. 410–412; 1943.
[8] Data supplied by Trans-Tech, Rockville, Md. (A. C. Blankenship, private communication), August 23, 1960.
[9] G. R. Jones, "Calculated Magnetic Fields of Ferrite, Rods, Discs, and Slabs," U. S. Dept. of Commerce, O.T.S. No. PB 131938; 1959.
[10] C. L. Hogan, "The elements of nonreciprocal microwave devices," Proc. IRE, vol. 44, pp. 1345–1368; October, 1956.